

Jacobian weighting of distortion corrected EPI data

S. Skare^{1,2}, and R. Bammer¹

¹Radiology, Stanford University, Stanford, CA, United States, ²MR Center, Clinical Neuroscience, Karolinska Institute, Stockholm, Sweden

Introduction: The Reversed Gradient Polarity Method ('RGPM')¹ has proven effective in correcting for geometric distortions in EPI data from two oppositely distorted magnitude EPI images, in particular when the estimation of smooth displacement fields are enforced via basis functions and optionally combined with simultaneous motion correction^{2,3}. This method does not involve extensive calibration measurements like in the case for the PSF method⁴, nor does it rely on measured field maps⁵, making it practical to use with minimal scan time increase. Yet, in areas where the brain anatomy has been compressed so much that many voxels are compressed into one, the RGPM method will fail, both in terms of how well the displacement field is estimated and the ability to resample the distorted EPI data back to its true voxel locations. Even with a hypothetically known displacement field, with image resampling alone, one cannot recreate this lost anatomic information from these areas, such as frequently seen at regions around the ear canals. Fortunately, wherever the signal pile-up occurs in one image (I_+), there is a corresponding stretch of the same anatomy in the oppositely distorted image (I_-) due to the phase-encoding blip reversal. To correct for the intensity changes associated with the distortion, the Jacobian modulation function is used (pixel-wise) to obtain the corrected data:

$$\begin{cases} I_{+,corr}(\mathbf{r}) = I_+(\mathbf{r} + \mathbf{d}(\mathbf{r})) (1 + D_v \mathbf{d}(\mathbf{r})) = I'_+ J_+ \\ I_{-,corr}(\mathbf{r}) = I_-(\mathbf{r} - \mathbf{d}(\mathbf{r})) (1 - D_v \mathbf{d}(\mathbf{r})) = I'_- J_- \end{cases} \quad [1]$$

Resampling at positions $\mathbf{r} \pm \mathbf{d}(\mathbf{r})$ Jacobian modulation

where D_v is the directional derivative of $\mathbf{d}(\mathbf{r})$ along direction $\mathbf{v} = [1,0]$ (phase, freq). As seen in Eq. [1], when the Jacobian modulation becomes negative, the image intensity becomes negative and the correction breaks down. Moreover, a Jacobian smaller than 1 indicates that the corresponding region is compressed and leads to loss of effective resolution.

Materials and Methods: In this work, we are proposing a better use of the $I_{+,corr}$ and $I_{-,corr}$ data than a simple averaging of the two, with the aim to increase the effective resolution and suppress residual pile-ups in the corrected data. Here, each image (I_+ , I_-) is weighted by the Jacobian information before combination according to:

$$I_{comb} = \frac{I_{+,corr} W_+ + I_{-,corr} W_-}{W_+ + W_-} ; W_{\pm} = \begin{cases} 0 & \text{if } J_{\pm} < T \\ (J_{\pm})^p & \text{if } J_{\pm} > T \end{cases} \quad [2]$$

where T is a threshold value, chosen here to be zero to filter out pixels where Eq. [1] yields negative numbers. For all other pixels where $J_{\pm} > T$, we weight the data with the square of J_{\pm} ($p=2$) to more strongly favor large J 's. For experimental verification, thirteen axial single-shot spin echo EPI slices were collected on a healthy volunteer on a GE 3T Discovery MR750 system equipped with a 50 mT/m, SR=200 T/m/s gradient system using an 8-channel head coil. Other relevant imaging parameters were: FOV = 28x28 cm, $\Delta z = 4$ mm, resolution 256x256, TE/TR = 60/6000 ms, partial Fourier (24 overscans). Images were distortion-corrected using the B-spline based algorithm described elsewhere^{3,6}, followed by the new image weighting provided in Eq. [2]. The separation of the 2D B-splines (i.e. the resolution of the $\mathbf{d}(\mathbf{r})$ field) was 25 mm.

Results: In Fig. 1a, the I_+ and I_- images are shown prior to correction, with pronounced pile-up regions right on top of the middle cerebral arteries for the I_- image, and in posterior part of the brain for the I_+ image. A difference image is given in the rightmost panel. In Fig. 1b, the corresponding data are shown after distortion correction, but before averaging of the two images. The low residuals remaining in Fig. 1b (right) suggests that the displacement field was well estimated. However, in the $I_{-,corr}$ image, the red nuclei (red arrows) are no more visible than prior to correction. Conversely, very poor resolution of the posterior anatomy (white arrows) is seen in the $I_{+,corr}$ image. In Fig. 2a, the weighting images, W_+ and W_- , computed from $\mathbf{d}(\mathbf{r})$ are shown using $p=2$ (Eq. [2]). Using these weighting images, we attempt to combine the most informative data from the two corrected images (Fig. 2b), and most anatomic regions are now shown with adequate resolution.

Discussion: While obtaining an accurate displacement field is the first step in RGPM-based distortion correction, the combination step of the two corrected images should not be neglected. The underlying concept of the new approach is that we trust stretched data more than compressed data, simply because more pixels are resampled into fewer pixels, retaining the final resolution after correction. While our choice of T and p in Eq. [2] worked well in our experiments, more data will show what values are most useful. T , for example, can be set to any value between 0 and 1. The value of p could on the other hand be set to any value larger than zero, with larger values meaning a stronger selection between the two images. Further improvements could also involve effective resolution measurements to produce even more reliable weighting maps. Also, it should be noted that even if our method pushes the distortion correction abilities further, we will not be able to correct for signal pile-up that has completely left the originating anatomy. This will happen for distortions larger than those presented here.

Acknowledgements: This work was supported in part by the NIH (5R01EB002711, 1R21EB006860, 1R01EB008706, 1R01EB006526), The Center for Advanced Technology at Stanford (P41RR09784), the Swedish Research Council (K2007-53P-20322-01-4), the Oak Foundation and the Lucas foundation.

References: [1] Chang, H. and J.M. Fitzpatrick, IEEE Trans Med Imag, 1992. **11**(3): p. 319-329. [2] Andersson, J.L.R., S. Skare, and J. Ashburner, Neuroimage, 2003. **20**(2): p. 870-88. [3] Skare, S. and J.L. Andersson, Magn Reson Med, 2005. **54**(1): p. 169-81. [4] Chen, N.K. and A.M. Wyrwicz, Magn Reson Med, 1999. **41**(6): p. 1206-13. [5] Jezard, P. and R.S. Balaban, Magn Reson Med, 1995. **34**(1): p. 65-73. [6] Skare, S., J.L.R. Andersson, and R. Bammer., ISMRM 2008, Toronto.

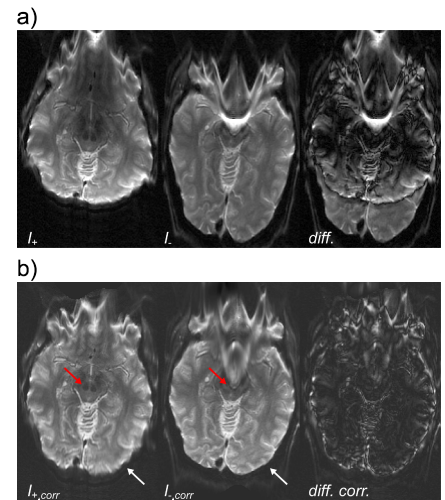


Figure 1. a) I_+ , I_- , and difference images before correction. b) Same images after correction. Even if the difference image indicates that a plausible field has been estimated, the effective resolution has changed in the images. The $I_{+,corr}$ image lacks resolution near the white arrow whereas the $I_{-,corr}$ image show artifacts near the red nuclei (red arrow).

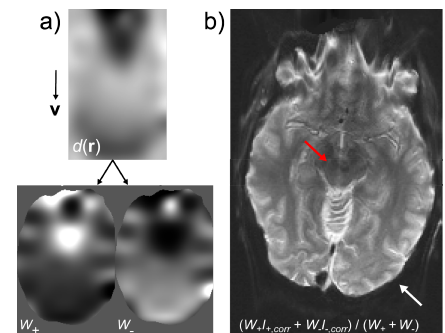


Figure 2. a) Estimated displacement map, with distortion direction vector \mathbf{v} (Eq. [1]), that is used to generate the weighting images W_+ and W_- (Eq. [2]). b) Proposed averaging of the corrected images using $p = 2$ and $T = 0$ (Eq. [2]).